Pharm Res (2014) 31:46–59
DOI 10.1007/s11095-013-1130-4

RESEARCH PAPER

Promoting Antitumor Activities of Hydroxycamptothecin by Encapsulation into Acid-Labile Nanoparticles Using Electrospraying

Xiaoming Luo • Guoqing Jia • Haixing Song • Chaoyu Liu • Guannan Wu • Xiaohong Li

Received: 15 December 2012 / Accepted: 24 June 2013 / Published online: 25 July 2013

ABSTRACT

Purpose Acid-labile nanoparticles are proposed to enhance the tumor targeting and anti-tumor therapy of hydroxycamptothecin (HCPT) in response to the acidic microenvironment within cells and tumor tissues.

Methods HCPT was entrapped into matrix polymers containing acid-labile segments and galactose moieties (PGBELA) through an electrospraying technique. The antitumor activities of HCPT-loaded nanoparticles were evaluated both on HepG2 cells and after intravenous injection into H22 tumor-bearing mice.

Results The electrosprayed nanoparticles were obtained with enhanced loading efficiency and extended release of HCPT compared with other nanoparticle preparation methods. The acid-lability and targeting capability of PGBELA nanoparticles resulted in a 5 times higher inhibitory activity after incubation in pH 6.8 media compared to that of pH 7.4. Animal studies indicated that both the blood circulation time and tumor distribution of PGBELA nanoparticles were significantly increased. HCPT/PGBELA nanoparticles indicated a superior *in vivo* antitumor activity and fewer side effects than other treatments on the basis of tumor growth, animal survival rate, tissue necrosis and cell apoptosis evaluation.

Conclusion Biodegradable PGBELA nanoparticles are capable of achieving site-specific drug delivery by active targeting and triggered release by acidic pH both in tumor tissues and after internalization within tumor cells, thereby providing a novel strategy for cancer treatment.

KEY WORDS acid lability · antitumor activity · biodistribution · electrosprayed nanoparticles · targeting capability

INTRODUCTION

Liver cancer is becoming one of the most harmful diseases and a significant threat to the public's health, and there are about 700,000 new cases per year globally (1). Liver transplantation or surgical resection has been clinically used in the treatment of primary liver cancer, but more than 80% of hepatocellular carcinoma patients are not eligible for surgical removal because their cancer is too advanced or easy to spread to another part of the body. Additional chemotherapy and biologic therapy has not been shown to improve overall survival for patients, making new therapeutic strategies an immediate need to combat liver cancer (2). Historically systemic administration of chemotherapeutic drugs like hydroxycamptothecin (HCPT), cisplatin, doxorubicin and 5-fluorouracil shows good efficacy for cancer treatment, but there are several limitations associated with cancer chemotherapy. One of the well-known drawbacks is the lack of selectivity to cancer cells leading to toxicity to many healthy tissues. Therefore, the incorporation of therapeutic drugs into nanocarriers, such as nanoparticles, liposomes, and micelles, has been

Electronic supplementary material The online version of this article (doi:10.1007/s11095-013-1130-4) contains supplementary material, which is available to authorized users.

X. Luo • G. Jia • C. Liu • G. Wu • X. Li (✉)
Key Laboratory of Advanced Technologies of Materials
Ministry of Education of China
School of Materials Science and Engineering Southwest Jiaotong University, Chengdu 610031
People's Republic of China
e-mail: xhli@swjtu.edu.cn

H. Song
Department of Biomedical Science, Chengdu Medical College
Chengdu 610083 People's Republic of China

explored to improve the accumulation of chemotherapeutic agents in tumor sites through the enhanced permeability and retention (EPR) effect, which results from the abnormalities of tumor blood and lymphatic vasculature (3). To further improve the delivery efficiency of the nanocarriers and efficacy of the drug after traveling into the extravascular space of the tumor, active targeting strategies have been achieved through coupling with specific ligands, such as vitamins, aptamers, lectins, carbohydrates, antibodies and their fragments. These ligands provide preferential accumulation of the nanocarriers in tumor tissues and cancer cells, and the receptor-mediated endocytosis enhances the cellular uptake and enrichment in specific cell organelles (4). The asialoglycoprotein (ASGP) receptors on the hepatocellular carcinoma cell membrane were able to specifically recognize β-D-galactose, which has been widely investigated as a target agent to promote the accumulation in the tissue and enhance the ligand-mediated cellular uptake and endocytosis (5).

The drug release from above nanocarriers is usually realized by a passive diffusion both at the target site and in the bloodstream during drug delivery, which becomes a major challenge to improve the therapeutic efficacy. It is optimal to achieve a rapid release upon reaching and accumulating in tumor tissues and after being taken up by cancer cells, while a minimal release during circulation in the bloodstream or in normal tissues. Therefore, the use of carriers responsive to stimuli, such as pH, temperature, and specific enzymes is another promising targeting approach (6). Studies on human patients and animal xenografts revealed that the average pH in the tumor environment (pHe) is in the range of 6.5 to 7.0 (with an average of 6.8), compared with normal tissue of 7.4, which is caused by up-regulated glycolysis and the production of lactate and protons in the extracellular microenvironments (7). There are also pH gradients in the intracellular endosomal compartments that reach pH levels of 5.0–6.5 (8). The heterogeneous variations of pH between normal and tumor tissues and inside cancer cells have often been targeted for therapeutic strategies in the area of drug delivery. One of the pH-triggered strategies entails the use of acid-labile functional groups that are less stable at tumor pHe. The cleavage of the acid-labile linkage results in either a decrease in matrix integrity and release of loaded drug, or an exposure of targeting ligands (9). Micelles, liposomes, hydrogels, and nanoparticles based on pH-sensitive polymers have been designed to deliver drugs for treating cancer using pHe as a stimulus (10). Duan *et al.* prepared chitosan-graft-poly(N-isopropylacrylamide) nanogels with the loading of oridonin, which displayed pH-dependent release behaviors and higher cytotoxicity at pH 6.5 than at pH 7.4 to HepG2 cells (11).

Nanoparticles are rapidly evolving as interesting and effective nanocarriers in cancer chemotherapy. Numerous methods exist for producing drug-loaded nanoparticles, such as solvent evaporation from single or double emulsions, nanoprecipitation, and spray drying. However, some inevitable limitations are associated with these methods. For example, emulsification methods usually result in a broad particle size distribution, low drug loading efficiency, low particle collection efficiency, and tedious separation procedures of nanoparticles. In addition, non-degradable additives such as surfactants and polymer stabilizers are often required as emulsifiers (12). Lee *et al.* indicated that the residual poly(vinyl glycol) around the obtained nanoparticles obstructed the diffusion of the encapsulated drug, and restricted the complete release of the drug (13). Electrospraying is an emerging technique for the rapid and high throughput preparation of particles in the nano- to micro-scale, and has potential advantages in cost and simplicity in the preparation of polymer particles (14). A strong electric field is applied during electrospraying to break up a polymer solution containing drugs into a stream of finely dispersed particles. The direct deposition of particles onto the collector under the electric field usually leads to high production efficiency, avoiding high shear forces and residual surfactant on the nanoparticle surface (15). In addition, electrospraying techniques can achieve a high loading capacity and uniform drug dispersion in particle matrices with minimal drug loss (16). Attempts have been made to examine the process parameters on the characteristics of electrosprayed nanoparticles, and evaluate preliminarily the efficacy of drug-loaded nanoparticles. Ding *et al.* loaded Taxol into polycaprolactone (PCL) microparticles with diameter of 1 −15 μm at a drug encapsulation efficiency of about 80% using electrospraying, demonstrating the applicability of the method for fabricating drug-carrying particles (17). Wu *et al.* fabricated doxorubicin-loaded nanoparticles through electrospraying, indicating that the morphologies of electrosprayed particles were greatly influenced by the molecular weight of the matrix polymers and the concentration of polymer solutions (18).

As a derivative of camptothecin, HCPT possesses much better antitumor efficacy against various solid tumors. But it has not been widely used in clinic due to its insolubility in water and in physiologically acceptable organic solvents. Further, the hydrolysis of the lactone ring under physiological conditions into an open carboxylate form compromises the anti-tumor activity (19). Up to now many non-pH-responsive formulations such as chemical conjugation, liposomes, micelles, hydrogels and electrospun fibers have been developed to improve the therapeutic efficacy and reduce the systemic cytotoxicity (19). In our previous study, acid-labile segments containing acetal groups were copolymerized with DL-lactide by bulk ring-opening polymerization, and galactose was conjugated onto above polymers through click chemistry. The breakdown of acetal linkages at mildly acidic pH resulted in

the acid lability of the obtained polymers. Acid-labile microspheres with the loading of pDNA polyplexes were obtained with the size of 2−3 μm by double emulsion solvent evaporation. Higher cellular uptake of microparticles and promoted transfection efficiency of pDNA were achieved on liver macrophages (20). In the current study, acid-labile nanoparticles were initially evaluated for the antitumor efficacy, to take advantage of the acid-lability, full biodegradable backbone and targeting capabilities of the matrix polymer and the acidic tumor pHe. HCPT-loaded nanoparticles were prepared by electrospraying to enhance the particle collection and drug loading efficiency. The drug release and polymer degradation profiles were investigated in buffer solutions of different pH values to reflect the responsiveness in the physiological pH 7.4, endosomal pH and tumor pHe. The cellular uptake and cytotoxicity of HCPT-loaded nanoparticles were examined *in vitro* on HepG2 cells, and the antitumor activities were evaluated on hepatic H22 tumor-bearing mice with respect to the animal survival, tumor growth and cell apoptosis.

MATERIALS AND METHODS

Materials

Galactose grafted poly(benzaldehyde-polyethylene glycol)-poly(DL-lactide) (PGBELA) was prepared through click reaction of poly(4-propargyl-benzaldehyde-poly(ethylene glycol))-poly(DL-lactide) with 1-O-2-azidoethyl-β-D-glactose (20). Poly(benzaldehyde-poly(ethylene glycol))-poly(D,L-lactide) (PBELA) was obtained by copolymerization of DL-Lactide with poly(benzaldehyde-poly(ethylene glycol)) (21). Poly(ethylene glycol)-poly(DL-lactide) (PELA) were prepared by bulk ring-opening polymerization of DL-lactide/poly(ethylene glycol) (PEG) using stannous chloride as the initiator (22). Copolymers PGBELA, PBELA and PELA indicated weight-average molecular weight (M_w) of 28.3, 30.6 and 29.3 kDa, and polydispersity indices (M_w/M_n) of 1.24, 1.21 and 1.31, respectively. HCPT was purchased from Sichuan Natural Product Co. (Chengdu, China) and stored at −20°C. All the electrophoresis reagents, bovine serum albumin (BSA) and 3-(4,5-dimethylthiazol-2-yl)-2,5-diphenyltetrazolium bromide (MTT) were procured from Sigma (St. Louis, MO). Protein molecular weight marker and RIPA lysis buffer were from Beyotime Institute of Biotechnology (Shanghai, China). Rabbit anti-human procaspase-3 antibody was purchased from Abcam Inc. (Cambridge, MA), and rabbit anti-mouse caspase-3 antibody, goat anti-rabbit IgG−horseradish peroxidase (HRP) and 3,3-diaminobenzidine (DAB) developer were purchased from Biosynthesis Biotechnology Co., Ltd. (Beijing, China). All other chemicals and solvents were of reagent grade or better, and purchased from Changzheng Reagents Co. (Chengdu, China) unless otherwise indicated.

Preparation of Drug-Loaded Nanoparticles by Electrospraying

HCPT-loaded PGBELA nanoparticles (HCPT/PGBELA) were prepared by electrospraying as described previously with some modifications (18). Briefly, HCPT was dissolved in dimethyl sulphoxide (DMSO) at 10.0 mg/ml, and PGBELA was dissolved in dimethyl formamide (DMF) at 50.0 mg/ml. The blend of polymer and HCPT solutions (15/1, v/v) was placed into a 5-ml syringe and was continuously pushed by a microinject pump (Zhejiang University Medical Instrument Co., Hangzhou, China) at a flow rate of 3.0 ml/h. A high-voltage power supply (Tianjing High Voltage Power Supply Co., Tianjing, China) was used to generate a 20 kV potential difference, and a spraying distance of 10 cm was set between the syringe nozzle with the size of 0.55 mm and the grounded copper foil, which was immersed in the collecting solution (20 ml) of water and ethanol (1/1, v/v). A stable electrospray was produced from a Taylor cone, and the nanoparticles were collected by centrifugation and stored away from light at 4°C after lyophilization. HCPT/PBELA and HCPT/PELA nanoparticles were prepared following the same procedures, and blank PELA, PBELA and PGBELA nanoparticles were prepared without the addition of HCPT.

Characterization of HCPT-Loaded Nanoparticles

Scanning electron microscopy (SEM, FEI Quanta200, The Netherlands) and transmission electron microscopy (TEM, Hitachi H-600-4, Japan) were used to observe the morphologies of the nanoparticles obtained. The particle size and zeta potential of nanoparticles were measured by a Nano-ZS laser particle analyzer (Zetasizer Nano ZS, Malvern Co., UK). The HCPT entrapment in nanoparticles were determined with a fluorescence microscope (Leica DMR HCS, Germany), which was operated with a Cy2 filter with the excitation wavelengths of 340−400 nm and emission wavelengths of 450−600 nm. The loading amount and encapsulation efficiency of HCPT were quantified by a fluorospectrophotometer (Hitachi F-7000, Japan) with the excitation wavelength of 380 nm and the emission wavelength of 550 nm after being extracted from nanoparticles as described previously (23).

In Vitro Drug Release and Matrix Degradation of HCPT-Loaded Nanoparticles

The acid-lability was determined from HCPT release and matrix degradation after incubating HCPT-loaded PGBELA, PBELA and PELA nanoparticles in phosphate buffer saline (PBS) of pH 7.4, 6.8 and 6.0 (23). Briefly, nanoparticles with the loading of around 120 μg HCPT

were immersed in buffer solutions, which were maintained in a shaking water bath at 37°C and 120 cycles/min. At predetermined time intervals the release media and nanoparticles were separated from the well dispersed nanoparticle suspensions by centrifugation. Small aliquots of release media were retrieved, and the amount of HCPT release was measured with a fluorospectrophotometer as mentioned above. In separate experimental groups the recovered nanoparticles were vacuum dried, and the mass loss was determined gravimetrically by comparing with the initial weight. The molecular weight of the recovered nanoparticles was determined by gel permeation chromatography (GPC, Waters 2695 and 2414, Milford, MA) using polystyrene as the standard.

Cytotoxicity of HCPT-Loaded Nanoparticles

The inhibition of cell growth was determined on HepG2 cells (American Type Culture Collection, Rockville, MD) after exposure to HCPT-loaded nanoparticles at pH 7.4 and 6.8. Briefly, HepG2 cells were cultured in pH 7.4 RPMI 1640 (Gibco BRL, Rockville, MD) containing 10% fetal bovine serum (FBS, Gibco Invitrogen, Grand Island, NY). The pH of the culture medium was adjusted to pH 6.8 with 0.1 M HCl, and no considerable pH drift in the culture medium was observed during the cytotoxicity tests. The cells were seeded at a density of 5000 cells/well in 96-well tissue culture plates (TCP), and allowed to attach and grow in wells for 24 h before drug treatment. Free HCPT and HCPT-loaded nanoparticles that released an equivalent amount of HCPT during 72 h (determined from *in vitro* release data) were applied (23), and the cell proliferation without drug treatment was set as the control. After incubation for 72 h the cell viability was determined by the MTT assay as described previously (20).

A procaspase-3 western blot was processed to investigate the cell apoptosis induced by HCPT-loaded nanoparticles. Briefly, HepG2 cells at a density of 5×10^5 per well were cultured in pH 6.8 and 7.4 media in 6-well TCP for 24 h. Cells were treated with free HCPT, empty and HCPT-loaded PGBELA, PBELA and PELA nanoparticles as above for 72 h, using untreated cells as the control. HepG2 cells were then incubated with RIPA lysis buffer, and the total proteins of the cell lysate were determined by BCA protein assay kit (Pierce, Rockford, IL). The proteins were separated by polyacrylamide gel electrophoresis and transferred to a poly(vinylidene fluoride) membrane (Immobilon-P, Millipore). The membrane was blocked with BSA, followed by incubation with procaspase-3 antibody at 4°C overnight. After incubation with secondary HRP-conjugated antibody for 1 h, the membrane was visualized with a DAB developer. Expression of β-actin was used as protein loading control.

Cellular Uptake of HCPT-Loaded Nanoparticles

The cellular uptake of nanoparticles was determined as described elsewhere with some modifications (24). Briefly, HepG2 cells were grown for 24 h on coverslips in a 24-well TCP, and then incubated with HCPT-loaded PGBELA, PBELA and PELA nanoparticles at a concentration of 4 μg/ml. In another experimental group galactose aqueous solution was added into the media prior to the addition of HCPT/PGBELA nanoparticles. After 4 h incubation, cells were fixed using 4% paraformaldehyde, and photographed using a confocal laser scanning microscope (CLSM, Leica TCS SP2, Germany). Cells were lysed by 50 μl 0.5% Triton X-100 for 2 h at 4°C, and the fluorescence intensity of the cell lysate was measured as above. The cellular uptake efficiency was obtained by comparing with the fluorescence intensity of the nanoparticles added.

Treatment of Tumor-Bearing Animals with HCPT-Loaded Nanoparticles

All animal procedures were approved by the University Animal Care and Use Committee. The tumors were established on Kunming mice (weighing 18–22 g, aged 6–8 weeks, Sichuan Dashuo Biotech Inc., Chengdu, China) by subcutaneous injection of mouse hepatoma H22 cells as described previously (23). The tumors were allowed to grow for around 10 days to reach the size of around 450 mm^3. Animals were treated by intravenous administration of free HCPT, HCPT-loaded PGBELA, PBELA and PELA nanoparticles with HCPT dose of 4.0 mg/kg body weight, using empty PGBELA, PBELA and PELA nanoparticles and saline as control. Nanoparticles were suspended in saline, while free HCPT was dissolved in PBS containing DMSO (5%, v/v), and each animal was administrated about 0.2 ml through the tail vein.

HCPT Biodistribution in Tumor-Bearing Mice

HCPT-loaded nanoparticles and free HCPT were administered into animals, and the HCPT distribution in different tissues was evaluated as described previously (24). Briefly, at predetermined time intervals (0.5, 4, 12, 24 and 48 h), blood were collected to get plasma samples, and the animals were sacrificed to retrieve heart, liver, spleen, lung, kidney and tumor tissues, which were homogenized with saline and acidified to pH 3.0 with acetic acid. HCPT was extracted from the plasma and tissue homogenates by incubation with a mixture of acetonitrile and methanol (1/1, v/v) to precipitate proteins. The fluorescence intensity of HCPT in the extract was measured with a fluorospectrophotometer, and calibrated by the extract efficiency. The calibration for each tissue were established separately, which was obtained by the

addition of known amounts of free HCPT to the plasma or homogenate of tissues from untreated animals.

Anti-Tumor Efficacy of HCPT-Loaded Nanoparticles

The day when treatments started was defined as day 0, and each group had 8 animals. The body weights, tumor volumes and survival rate of animals were monitored every other day after treatment. The length of the major axis (longest diameter) and minor axis (perpendicular to the major axis) of the tumor were measured with a vernier caliper, and the tumor volume was calculated as described previously (23). The number of live animals at each time point was plotted in Kaplan Meier survival curves, and a 50% mean survival time was obtained for comparison of treatment efficacy. At day 20 after treatment, one animal from each group were randomly chosen and euthanized to retrieve tumors. The excised tumors were washed by saline, dried with filter paper, weighed and photographed before fixation in 10% neutral buffered formalin. Hematoxylin and eosin (HE) staining was performed routinely on tissue sections, and observed with a light microscope (Nikon Eclipse E400, Japan). Immunohistochemical (IHC) staining of caspase-3 expression was conducted to investigate the apoptosis of tumor cells as described previously (23). The expression levels of caspase-3 were compared by counting the apoptotic cells/100 cells of five tissue sections.

Statistics Analysis

The statistical significance of the data obtained was analyzed by the Student's *t*-test. Data are expressed as mean ± standard deviation (S.D.). Probability values of $p<0.05$ were interpreted as denoting statistical significance.

RESULTS AND DISCUSSION

Characterization of Electrosprayed HCPT-Loaded Nanoparticles

Figure 1a and b show the typical SEM and TEM morphologies of HCPT-loaded PGBELA nanoparticles, indicating a distinct spherical shape and smooth surface with an average size of around 200 nm. As shown in Fig. 1c, all the nanoparticles emitted blue fluorescent light, suggesting the presence of HCPT in nanoparticles. During the electrospraying process, others have commonly used a grounded steel plate or aluminum-foil to collect electrosprayed particles (25). In the current study, to achieve a better separation from nonencapsulated HCPT, a grounded copper foil immersed in water and ethanol (1/1, v/v) was used to collect electrosprayed nanoparticles. In addition, to determine the acid lability and targeting capabilities of nanoparticles from different matrix polymers, the particle size and drug loading amount of HCPT-loaded PELA, PBELA and PGBELA nanoparticles were designed to be very similar. Therefore, an orthogonal experimental design was applied to quantitatively evaluate and statistically analyze the effects of solution properties and processing parameters on the nanoparticle properties, which is provided in the Supplementary Material.

Table I summarizes the particle size, zeta potential and HCPT loading amount of the nanoparticles obtained. There was no significant difference among any of the parameters ($p>0.05$). The obtained nanoparticles had diameters of 200 −300 nm, ensuring efficient cellular uptake (26). It should be noted that the average size of nanoparticles dispersed in water measured by laser diffraction was slightly larger than those of dried nanoparticles observed by SEM and TEM. Electrostatic charges were created on nanoparticles during electrospraying to ensure a good dispersion (27), and the zeta potentials of around −20 mV could prevent the aggregation of nanoparticles in buffer solutions by the strong repellent forces among particles (28). Derakhshandeh *et al.* encapsulated 9-nitrocamptothecin into poly(DL-lactide-co-glycolide) (PLGA) nanoparticles with a size of around 210 nm by nanoprecipitation, indicating an optimal loading efficiency of about 33% (29), which was significantly lower than those of electrosprayed nanoparticles (Table I). The electrosprayed liquid droplets were rapidly solidified into nanoparticles while traveling to the collector, resulting in high drug loading efficiency. In addition, during the solvent evaporation from emulsion and nanoprecipitation processes, the leakage of hydrophilic drugs into the dispersion phase led to low drug loadings into nanoparticles obtained (30). Therefore, electrospraying should offer more advantages in the loading of hydrophilic compounds into nanoparticles to promote the encapsulation efficiency.

In Vitro HCPT Release from Electrosprayed Nanoparticles

The HCPT release behaviors from PGBELA, PBELA and PELA nanoparticles were investigated under a simulated physiological condition of pH 7.4 and in acidic buffers of pH 6.0 and 6.8, representing the endosomal pH and tumor pHe, respectively (31). Figure 2 shows the *in vitro* release profiles of HCPT-loaded nanoparticles under these different pH conditions. HCPT-loaded PELA nanoparticles showed similar release behaviors in buffers of pH 7.4, 6.8 and 6.0, indicating around 23% of burst release during 24 h incubation. The amount of sustained release was quite low during the following incubation, at around 34%, 38% and 40% after 24 days of incubation in pH 7.4, 6.8 and 6.0 buffers, respectively (Fig. 2a). As shown in Fig. 2b and c, there was 40.2 ± 1.8% and 43.2 ± 2.0% of HCPT release from

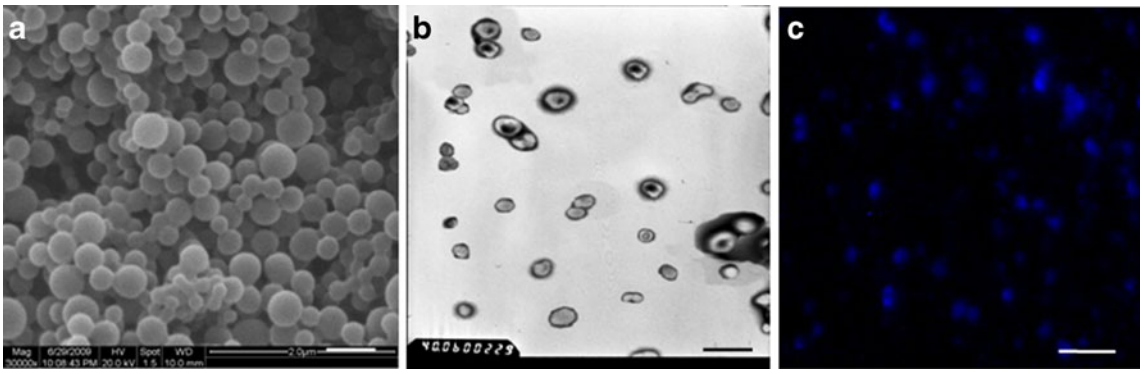

Fig. 1 (**a**) SEM, (**b**) TEM and (**c**) fluorescence microscope images of HCPT/PGBELA nanoparticles. *Bars* represent 500 nm.

PBELA and PGBELA nanoparticles after incubation in pH 7.4 for 24 days, which was close to that from HCPT/PELA nanoparticles. However, over 90% of HCPT release from PBELA and PGBELA nanoparticles was found after incubation for 24 days in pH 6.8 and 6.0. In addition, after incubation for 24 h in pH 6.8, HCPT/PGBELA showed an initial burst release of 48.8 ± 2.3% (Fig. 2c), which was significantly higher than 38.8 ± 1.6% of HCPT/PBELA nanoparticles (Fig. 2b).

HCPT-loaded polymer nanoparticles or liposomes always exhibit a significant burst release during the initial incubation, and it is one of the challenges to maintain the drug concentration within a therapeutic window during a sufficient exposure time. Miura *et al.* loaded camptothecin into methoxyl poly(ethylene glycol)–poly(DL-lactide) nanoparticles with a size of around 250 nm using conventional emulsification–evaporation method, indicating that more than 90% of the loaded drug was released in 24 h (32). Even PCL nanoparticles, which were considered to be slowly degrading and hydrophobic delivery materials, released almost 100% of the loaded camptothecin after 72 h (33). The sustained and slower release of electrosprayed nanoparticles may be attributed to the fact that the drug was uniformly dispersed within the polymeric matrix (16). In addition, acidic pH is a common characteristic of human tumors, and the increased acidity may be in fact essential in the progression of tumor growth and metastasis formation (34). As shown in Fig. 2, HCPT-loaded PGBELA and PBELA nanoparticles indicated larger initial burst release and higher sustained release rate in acidic buffers than those in neutral buffers. The acid-lability provided the targeted release of HCPT in response to the tumor stages of development, which was beneficial to enhance the bioavailability of antitumor agents in tumors while minimizing the exposure to normal tissues.

In Vitro Degradation of HCPT-Loaded Nanoparticles

The degradation behavior of HCPT-loaded nanoparticles was evaluated with respect to the mass loss, molecular weight change and molecular weight polydispersity of the matrix polymers. As shown in Fig. 3a, about 7−11% of mass loss was found for PELA particles after incubation for 24 days in buffer solutions of pH 7.4, 6.8 and 6.0, respectively, and there were no significant difference among them ($p>0.05$). However, about 20.9% and 23.5% of mass loss were detected for HCPT-loaded PBELA and PGBELA particles, respectively, after incubation for 24 days in pH 6.8. The mass loss became more significant in pH 6.0, at 25.0% and 26.7% for HCPT-loaded PBELA and PGBELA nanoparticles, respectively. Figure 3b shows the molecular weight reduction of matrix polymers of nanoparticles. PELA nanoparticles indicated about 10% of molecular weight loss in these buffer solutions, and similar results were found for HCPT-loaded PBELA and PGBELA nanoparticles after incubation in pH 7.4. However, the incubation of HCPT-loaded PBELA and PGBELA nanoparticles in acidic buffers led to significantly higher molecular weight reduction than that of HCPT/PELA nanoparticles. PBELA nanoparticles indicated around 21.7% and 26.3% of molecular weight loss after incubation for 24 days in pH 6.8 and 6.0, respectively. The molecular weight loss of HCPT/PGBELA nanoparticles was around 24.5% and 29.0% after incubation in pH 6.8 and 6.0, respectively. A previous study indicated that the

Table I Characterization of Electrosprayed HCPT-Loaded Nanoparticles

Nanoparticles	Particle size (nm)	Particle collection efficiency (%)	Zeta-potential (mV)	Loading amount (%)	Loading efficiency (%)
HCPT/PELA	258 ± 25	74.9 ± 7.8	−24.1 ± 1.9	1.03 ± 0.02	78.7 ± 4.4
HCPT/PBELA	235 ± 23	78.3 ± 6.4	−20.4 ± 1.3	1.05 ± 0.05	80.5 ± 4.5
HCPT/PGBELA	229 ± 25	74.3 ± 4.8	−17.6 ± 1.2	1.15 ± 0.07	83.6 ± 5.8

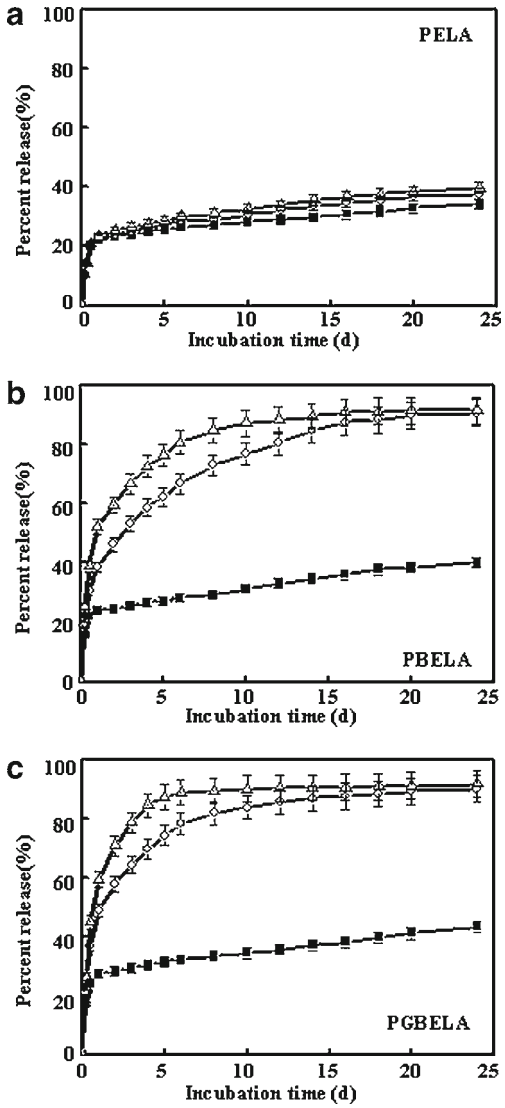

Fig. 2 Percent release of HCPT from (**a**) PELA, (**b**) PBELA and (**c**) PGBELA nanoparticles after incubation in buffer solutions of 7.4 (*black square*), 6.8 (*white circle*) and 6.0 (*white triangle*) at 37°C ($n = 3$).

degradation of PGBELA under acidic buffers initially occurred on acetal linkages of triblock copolymers, followed by the removal of galactose grafts and breakdown of polylactide segments (20). Figure 3c shows the increase in the molecular weight polydispersity for HCPT-loaded nanoparticles. The molecular weight polydispersity of HCPT/PGBELA nanoparticles increased from 1.40 to 1.62 after incubation in pH 6.8, and to 1.67 after incubation in pH 6.0 for 24 days.

As indicated above, the incubation of HCPT-loaded nanoparticles in pH 7.4 showed similar degradation behaviors, but PBELA and PGBELA nanoparticles showed a higher degradation rate under acidic conditions, indicating excellent acid-lability. In addition, PGBELA nanoparticles showed higher degradation rate than PBELA, due to the hydrophilic galactose grafts of PGBELA. The enhanced matrix degradation was responsible for the larger initial burst release and higher release rate of HCPT-loaded PGBELA nanoparticles after incubation in acidic buffers compared to PBELA nanoparticles (Fig. 2).

In Vitro Cellular Uptake of HCPT-Loaded Nanoparticles

HepG2 cells with the expression of ASGP receptor were used to evaluate the cellular uptake treated with different HCPT-loaded nanoparticles. As shown in Fig. 4a, there was no significant difference between HCPT/PELA and HCPT/PBELA nanoparticles with the uptake efficiency of around 32% ($p > 0.05$). Significantly higher cellular uptake efficiency of over 50% was detected for HCPT/PGBELA nanoparticles after incubation with HepG2 cells ($p < 0.05$), which may be mediated by galactose grafts through the ASGP receptor-mediated endocytosis. In order to confirm this observation, free galactose was added to the cell suspension 30 min prior to the addition of nanoparticles. As shown in Fig. 4a, the uptake efficiency of HCPT/PGBELA nanoparticles into HepG2 cells was significantly decreased to around 32%. Figure 4b shows the CLSM images of cellular uptake of HCPT/PGBELA nanoparticles, which appeared to be taken up by endocytosis and localized in cytoplasm as evident by the distribution of blue fluorescence. The decrease in the fluorescent intensity after the addition of free galactose reflected the competitive binding of free galactose and galactose decorated nanoparticles with HepG2 cells. Therefore, HCPT/PGBELA nanoparticles can take advantage of their passive targeting, due to the acid sensitivity to tumor environment, and active targeting, due to receptor-mediated endocytosis, to improve the target therapy of liver cancer.

In Vitro Cytotoxicity of HCPT-Loaded Nanoparticles

In the current study, the *in vitro* cytotoxicity of HCPT-loaded nanoparticles on HepG2 cells was tested at both pH 6.8 and 7.4. The cell survival rates were over 92% after incubation with empty PGBELA, PBELA and PELA nanoparticles of up to 1.0 mg/ml. Figure 5a summarizes the cell viability incubated with HCPT-loaded nanoparticles during 72 h, and the half maximal inhibitory concentration (IC50) was determined to show the effectiveness to inhibit the growth of tumor cells. The IC50 of free HCPT was 1.43 and 1.23 μg/ml when incubated with media of pH 7.4 and 6.8, respectively. But the IC50s of HCPT/PELA nanoparticles when incubated in pH 7.4 and 6.8 media were 0.798 and 0.595 μg/ml, respectively, which were about 2-fold lower than those of free HCPT. The encapsulation into nanoparticles was supposed to protect the structural integrity of HCPT (35), resulting in the increased cytotoxicity at both pH 7.4 and 6.8 compared with free drug. As shown in Fig. 5a,

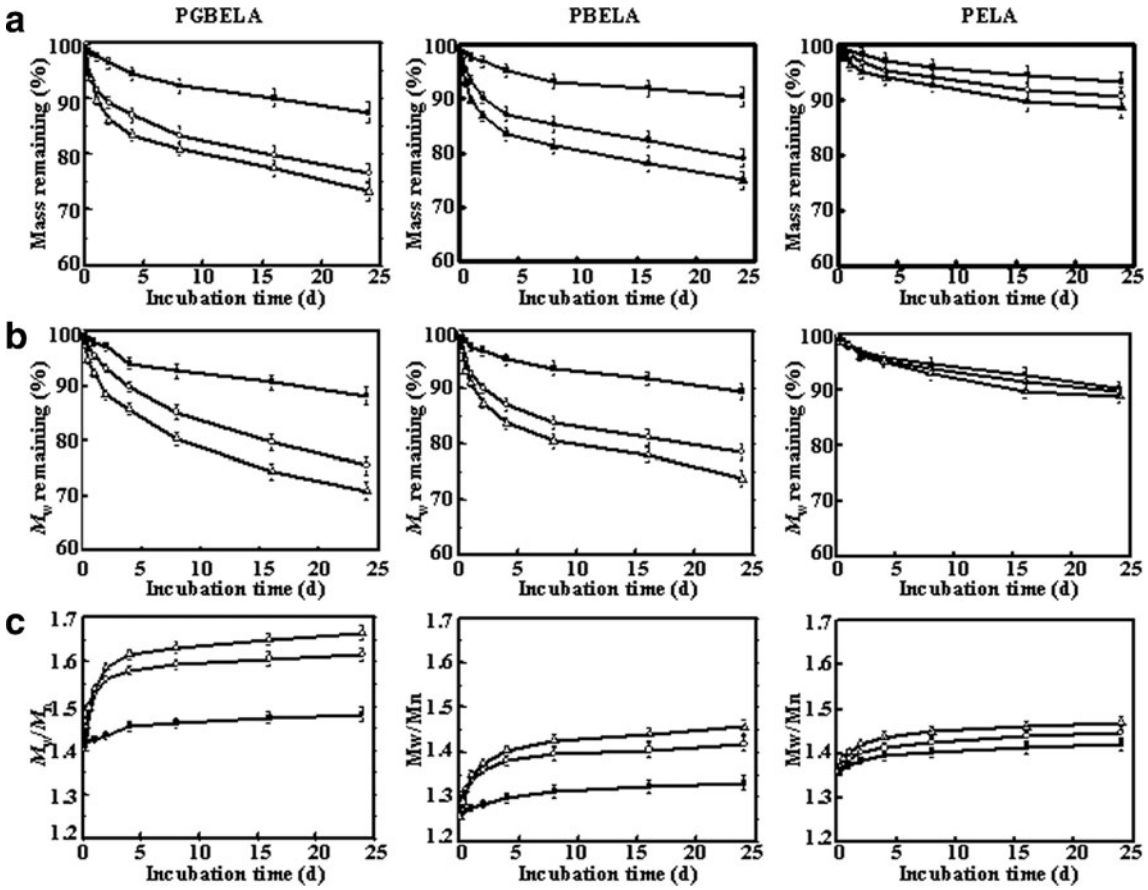

Fig. 3 (**a**) The mass remaining, (**b**) molecular weight remaining, and (**c**) molecular weight polydispersity increase of HCPT-loaded PGBELA, PBELA and PELA nanoparticles after incubation in buffer solutions of pH 7.4 (*black square*), 6.8 (*white circle*) and 6.0 (*white triangle*) at 37°C ($n = 3$).

the IC50s of HCPT/PBELA nanoparticles were 0.587 and 0.204 μg/ml, and those of HCPT/PGBELA nanoparticles was 0.407 and 0.083 μg/ml when incubated in pH 7.4 and 6.8 media, respectively, indicating 3−5 fold lower IC50s after incubation in pH 6.8 than those in pH 7.4 media. Considering that an equivalent amount of HCPT was dosed in the cell viability tests for each nanoparticle formulation, the pronounced cytotoxicity of acid-labile nanoparticles relied on the drug release profiles. This may be partially attributed to the accelerated release of HCPT triggered by low pH both in culture media and endosome after internalization within cells. Furthermore, HCPT/PGBELA nanoparticles indicated over 2-fold lower IC50 against HepG2 cells than HCPT/PBELA during 72 h incubation in pH 6.8 media. It should be attributed to the significantly higher uptake efficiency of PGBELA nanoparticles into cells (Fig. 4) and slightly higher release rate of HCPT from PGBELA nanoparticles in acidic solutions (Fig. 2).

It has been reported that the caspase activation is an important step to induce apoptosis in human hepatoma tumor cells by camptothecin treatment (36). Western blot of procaspase-3, the proform of active caspase-3 in HepG2 cells was used to examine the capability to induce apoptosis by HCPT-loaded nanoparticles (37). As shown in Fig. 5b, compared to empty nanoparticles and control group, HCPT-loaded nanoparticles and free HCPT resulted in decreases in the procaspase-3 levels of cells when incubated in pH 7.4 media. Moreover, when incubated under pH 6.8, HCPT/PGBELA nanoparticles showed the strongest apoptosis induction capabilities by prominent decrease of procaspase-3 among the experimental groups.

Biodistribution of HCPT in Tumor-Bearing Mice

An optimal distribution of anticancer agents *in vivo* is essential to improve the drug efficacy and, at the same time, to reduce side effects. Figure 6 summarizes the distribution of HCPT in major tissues for 48 h after intravenous injection of either free HCPT or HCPT-loaded nanoparticles into H22 tumor-bearing mice. As shown in Fig. 6a, HCPT accumulation in tumors reached a higher level after 12 h injection of HCPT/PGBELA nanoparticle than after injection of HCPT/PBELA, HCPT/PELA nanoparticles or free HCPT (38). At 48 h after injection, HCPT/PGBELA nanoparticles showed 2.4, 2.7 and 6.4 times higher accumulation in tumors compared to HCPT/PBELA, HCPT/PELA nanoparticles and free HCPT, respectively.

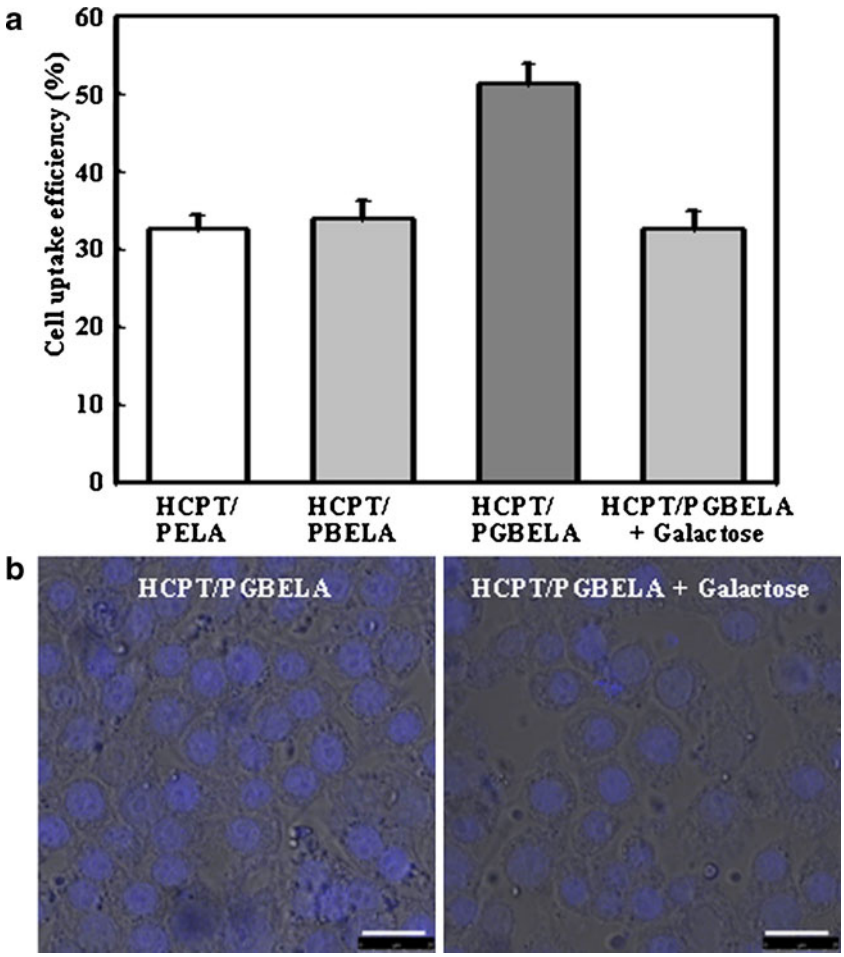

Fig. 4 (**a**) The uptake efficiency of HepG2 cells after incubation for 4 h with HCPT/PELA, HCPT/PBELA and HCPT/PGBELA nanoparticles. To test the galactose mediated targeting, 0.08 mol/l galactose solution was added to the cell suspension 30 min prior to the addition of HCPT/PGBELA nanoparticles ($n = 5$). (**b**) CLSM images of HepG2 cells after incubation with HCPT/PGBELA nanoparticles with or without the addition of galactose solution. *Bars* represent 20 μm.

This can be attributed to the receptor-mediated targeting (Fig. 4), and the accelerated release of HCPT from PGBELA nanoparticles in response to the acidic environment of solid tumors. As shown in Fig. 6b, HCPT concentrations in plasma

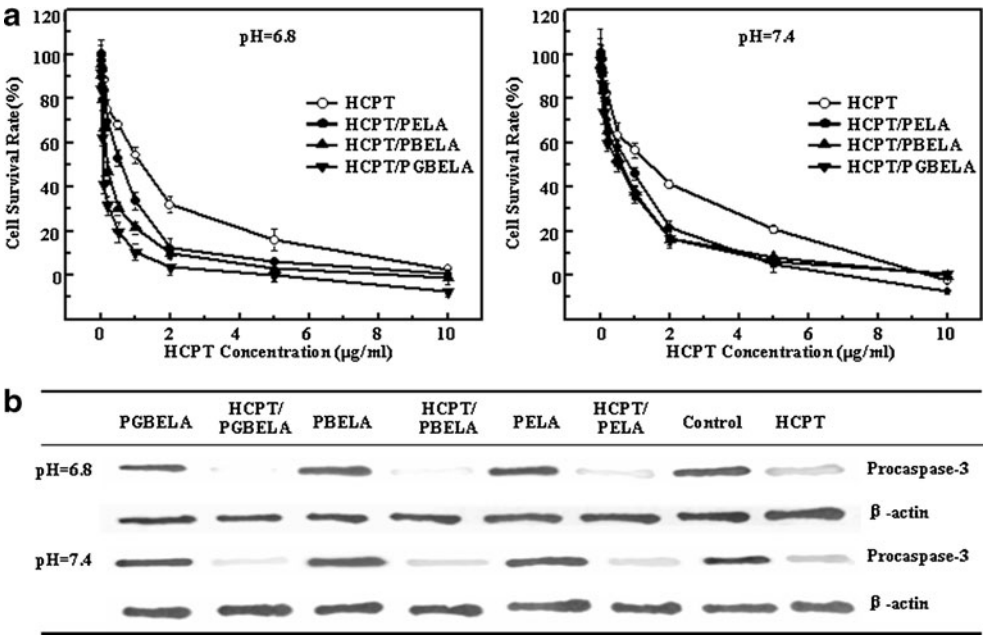

Fig. 5 (**a**) *In vitro* cytotoxicity to HepG2 cells (normalized to cells without treatment) after incubation in media of pH 7.4 and 6.8 and treated by free HCPT (*white circle*), HCPT-loaded PELA (*black circle*), PBELA (*black triangle*) and PGBELA nanoparticles (*black down pointing triangle*) ($n = 5$). (**b**) Western blot of procaspase-3 extracted from HepG2 cells after incubation in media of pH 7.4 and 6.8 and treated by free HCPT, HCPT-loaded PELA, PBELA and PGBELA nanoparticles, and empty PELA, PBELA and PGBELA nanoparticles, using untreated cells as control. Total proteins were prepared from cell lysate, and β-actin was used as protein loading control.

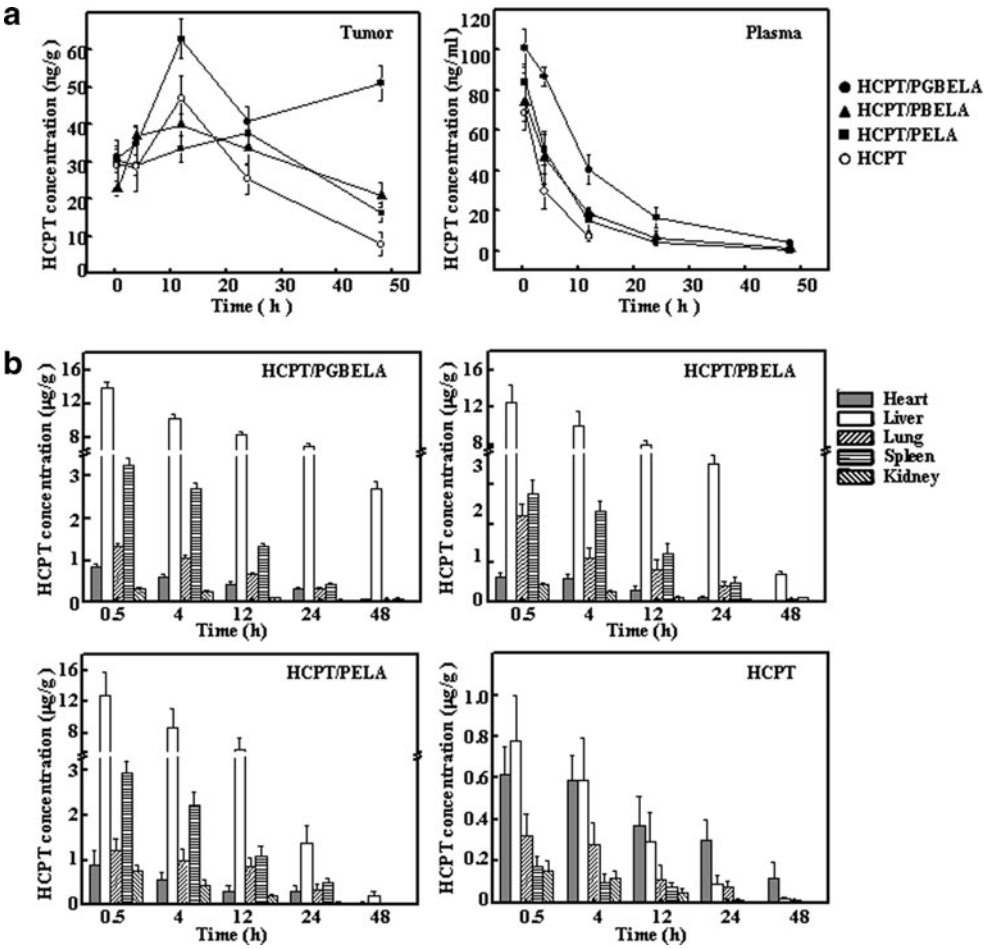

Fig. 6 (**a**) HCPT concentrations in tumor and plasma, and (**b**) HCPT concentrations in heart, liver, lung, spleen and kidney of H22 tumor-bearing mice after treatment with HCPT-loaded PGBELA, PBELA and PELA nanoparticles, and free HCPT.

decreased with time for both HCPT-loaded nanoparticles and free HCPT, and was detectable only during the first 12 h for free HCPT. At 24 h after injection, HCPT concentrations in plasma were 16.5, 6.49 and 4.36 ng/ml for HCPT-loaded PGBELA, PBELA and PELA nanoparticles, respectively. The prolonged retention period of HCPT levels in blood for nanoparticle samples was partly due to the constant release of HCPT from nanoparticles and the long circulation of nanoparticles (35). As shown in Fig. 6b, compared with HCPT-loaded PBELA and PELA nanoparticles, HCPT/PGBELA nanoparticles had an extended retention time in systemic circulation, due to the presence of hydrophilic galactose grafts on the nanoparticle surface (39). This was crucial to promote a site-specific delivery of HCPT/PGBELA nanoparticles into tumors mediated by galactose targeting groups. Thus the increased residence of HCPT/PGBELA nanoparticles in systemic circulation resulted in the remarkable increase in HCPT levels in tumors at 48 h after injection (Fig. 6a). Figure 6c shows the distribution of HCPT in heart, liver, spleen, lung and kidney, indicating higher accumulation of HCPT-loaded nanoparticles in these tissues compared to free HCPT. The colloid nature and a relative large diameter of around 230 nm of HCPT-loaded nanoparticles enhanced the uptake efficiency by reticuloendothelial system (RES) organs such as the liver and spleen (40). As shown in Fig. 6c, a high HCPT concentration accumulated in the livers of mice treated with HCPT/PGBELA nanoparticles, which was a result of their ability to target ASGP receptors on the membranes of hepatocytes and liver macrophages. Additionally, the HCPT concentration in the lung was found to be several times higher for the nanoparticles than free HCPT, due to the filtration effect of the lung capillary bed (41).

In Vivo Antitumor Efficacy

The antitumor efficacy of HCPT-loaded nanoparticles was evaluated with respect to the inhibition of tumor growth and development, and the survival rate of animals. Figure 7a summarizes the tumor growth curves after treatment with HCPT-loaded nanoparticles, empty nanoparticles, free HCPT and saline as the control. The subcutaneous tumors grew rapidly, and the tumor volume indicated an over 9-fold increase after 20 days in the saline group. There was no significant difference in the tumor volumes of mice treated with empty PELA, PBELA and PGBELA nanoparticles ($p > 0.05$). The tumor volume reached about 3650 mm^3 after

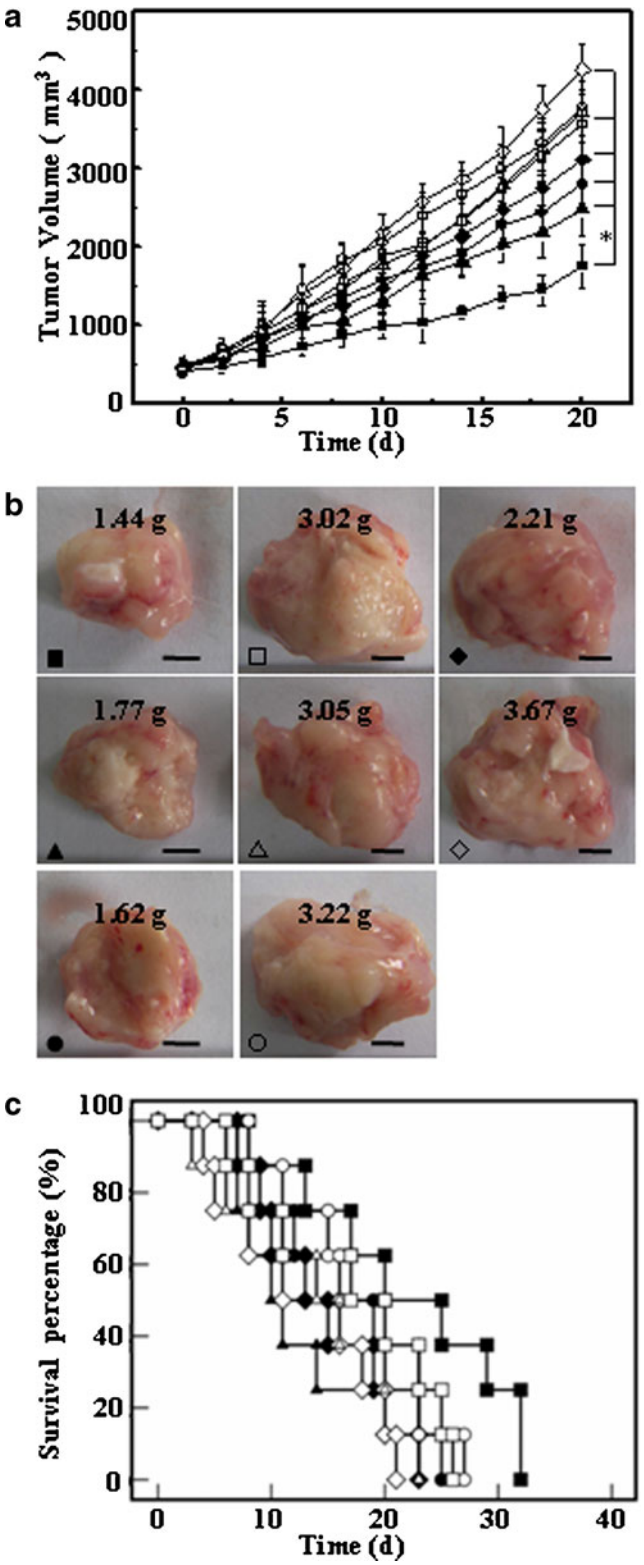

Fig. 7 (**a**) Tumor volume, (**b**) tumor weight on day 20 (*numbers* indicate the tumor weight, *bars* represent 5 mm), and (**c**) survival curve of H22 tumor-bearing mice after treatment with HCPT-loaded PGBELA (*black square*), PBELA (*black triangle*) and PELA nanoparticles (*black circle*), free HCPT (*black diamond*), empty PGBELA (*white square*), PBELA (*white triangle*) and PELA nanoparticles (*white circle*), and saline (*white diamond*) as the control. *: $p < 0.05$.

20 days of treatment, which was slightly smaller than the saline group, indicating no significant effect of empty nanoparticles and their degradable products on the tumor growth. The mean tumor volumes after 20 days of treatment with free HCPT, HCPT/PELA, HCPT/PBELA and HCPT/PGBELA nanoparticles were 3105, 2790, 2470 and 1743 mm^3, which was a 590%, 520%, 450% and 280% increase over the size before treatment, respectively. As shown in Fig. 7a, the increase in the tumor volume of mice treated with free HCPT for 12 days became accelerated compared with HCPT/PELA nanoparticles. The continuous inhibition of tumor growth in the nanoparticle groups was due to the sustained release of HCPT from nanoparticles and the retention of structural integrity of HCPT released from nanoparticles (35). The rapid tumor growth led to an increased acidity in the solid tumors, which enhanced the degradation of acid-labile PBELA and PGBELA nanoparticles (Fig. 3) and promoted the drug release (Fig. 2), leading to the significant inhibition of tumor growth compared with those of HCPT/PELA nanoparticles ($p<0.05$). The tumor growth was significantly inhibited after treatment with HCPT/PGBELA nanoparticles during the observation period compared with that of HCPT/PBELA nanoparticles. This was also in accordance with the increased accumulation of HCPT in the tumor (Fig. 6), enhanced cellular uptake (Fig. 4) and triggered drug release in response to the low pH environment in tumor tissues and intracellular compartment (Fig. 2). As shown in Fig. 7b, the tumor weight at the time of euthanasia showed the same trend. The animals treated with HCPT/PGBELA nanoparticles had the lowest tumor weight among all the treatment groups, demonstrating the greatest inhibitory effect on tumor growth.

The burden of tumor growth and systemic toxicity determined the survival period of animals. Figure 7c summarizes the survival rates of tumor-bearing mice from different treatment groups. HCPT/PGBELA nanoparticles extended survival of mice compared to other groups ($p<0.05$), and the 50% mean survival time was 20 days, which was resulted from the lower burden of tumor growth. The large tumor size after treatment with empty nanoparticles and the high systemic toxicity of free HCPT resulted in the 50% mean survival time of 13−14 days. The gradual release of HCPT from PELA and PBELA nanoparticles resulted in longer survival rates with the 50% mean survival time of 16−17 days.

Histological and IHC Evaluations of Tumors Retrieved

In order to clarify the antitumor efficacy of HCPT-loaded nanoparticles, tumor tissues were retrieved after 20 days of treatment for histological and IHC evaluations. Necrosis within tumors represents a significant prognostic factor of tumor volume after chemotherapy and the survival of patients (42). As shown in the representative HE staining images (Fig. 8a), a large amount of living cells (blue area) were

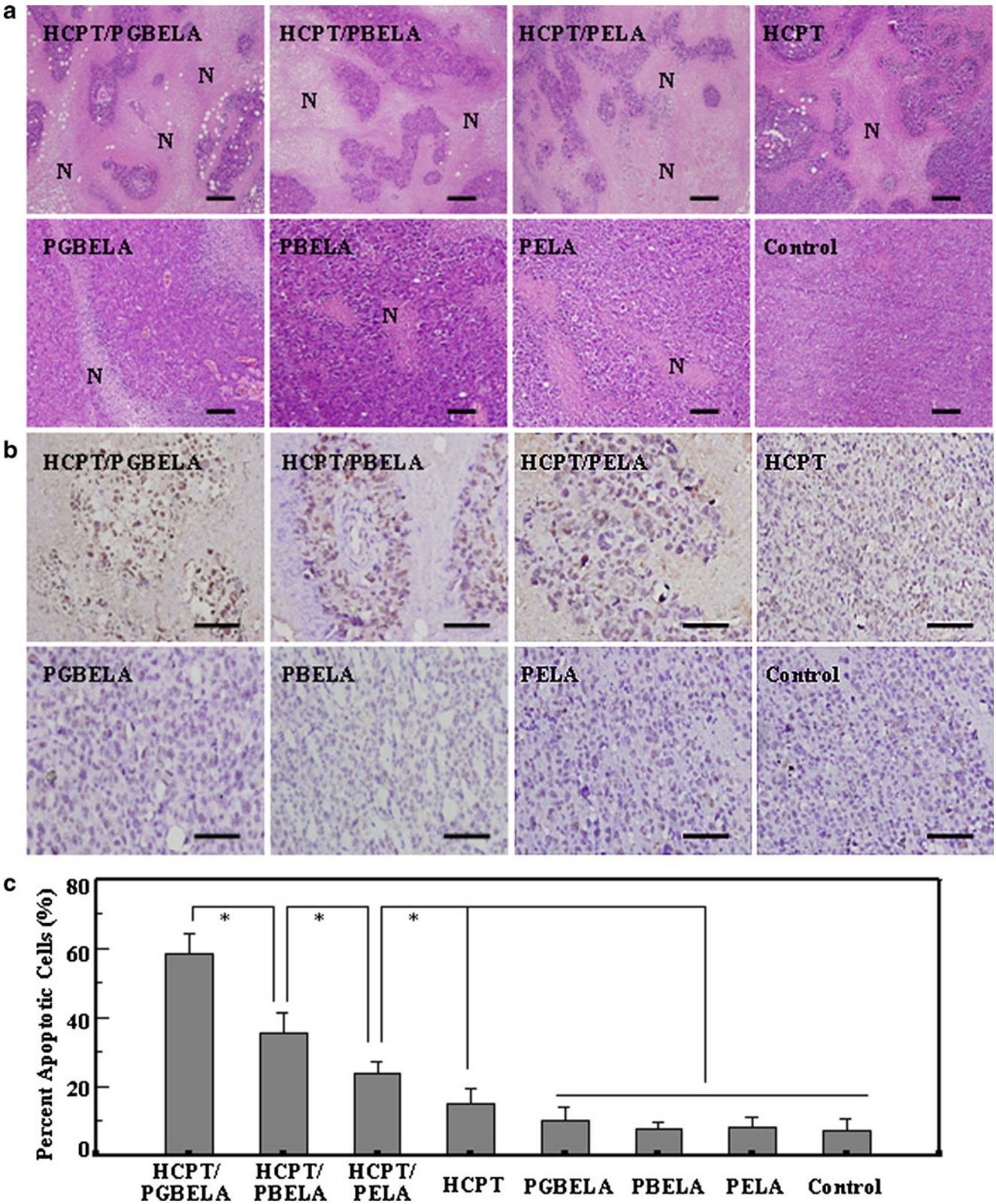

Fig. 8 (**a**) Typical HE staining images, (**b**) IHC staining images of capase-3, and (**c**) percentage of apoptotic cells in tumors retrieved on day 20 after treatment with HCPT-loaded PGBELA, PBELA and PELA nanoparticles, free HCPT, empty PGBELA, PBELA and PELA nanoparticles, and saline as the control. N represents necrotic area. *: $p < 0.05$. *Bars* represent 20 μm.

present in tumors and showed obvious nucleolus cleavage and high extent of malignancy after treatment with empty nanoparticles. Necrotic region (pink area) can be obviously seen in tumors after treatment with HCPT-loaded nanoparticles and free HCPT. As shown in Fig. 8a, the necrotic area in the tumor after treatment with HCPT/PGBELA nanoparticles was larger than other groups, indicating the effectiveness of nanoparticle accumulation within tumor tissues and sustained release of HCPT from PGBELA nanoparticles within the acidic environment of solid tumors.

The caspase family has been found to play a crucial role in the execution of apoptosis, in which caspase-3 plays a central role (43). As shown in the IHC staining profiles (Fig. 8b), the caspase-3 expressions were stronger in tumors after treated with HCPT-loaded nanoparticles and free HCPT than those of empty nanoparticles and control. Figure 8c summarizes the percent of apoptotic cells in tumors of different treatment groups. HCPT-loaded nanoparticles induced a significantly higher amount of apoptotic cells than free HCPT ($p<0.05$), due to the local and gradual delivery of HCPT into tumors. The enhanced release of HCPT from PBELA and PGBELA nanoparticles in response to the acidic tumor environment led to more apoptotic cells compared with HCPT/PELA nanoparticles ($p<0.05$). The preferred accumulation and uptake of HCPT/PGBELA nanoparticles into tumor cells induced the most significant apoptosis among the treatment groups, indicating the potential of acid-labile nanoparticles containing targeting moieties to improve the efficacy of antitumor treatment.

CONCLUSIONS

HCPT-loaded acid-liable nanoparticles were obtained through electrospraying with an average diameter of 230 nm. The electrosprayed nanoparticles indicated enhanced drug loading efficiency and extended release of HCPT compared with other nanoparticle preparation methods. The promoted uptake of PGBELA nanoparticle into HepG2 cells and accumulation into tumors of H22 tumor-bearing mice indicated the targeting capability of galactose moieties. Both the acid-lability and targeting capability of PGBELA nanoparticles resulted in a 5 times lower IC50 after incubation in pH 6.8 media than that of pH 7.4. The tumor growth, tissue necrosis, cell apoptosis and animal survival rate after intravenous injection of HCPT-loaded PGBELA nanoparticles indicated a superior *in vivo* antitumor activity and fewer side effects than other treatments. Electrosprayed PGBELA nanoparticles suggest a new strategy to achieve high chemotherapeutic efficacy through active targeting to tumor sites and stimuli-responsive drug release triggered by acidic pH both in tumor tissues and after internalization within tumor cells.

ACKNOWLEDGMENTS AND DISCLOSURES

Xiaoming Luo and Guoqing Jia contributed equally to the work. The authors thank Dr. Manfred F. Maitz from Max Bergmann Center of Biomaterials Dresden, Leibniz Institute of Polymer Research Dresden for his useful comments and language editing. This work was supported by National Natural Science Foundation of China (51073130 and 21274117), Specialized Research Fund for the Doctoral Program of Higher Education (20050613025 and 20120184110004), and Scientific and Technical Supporting Programs of Sichuan Province (2013SZ0084).

REFERENCES

1. Huynh H. Molecularly targeted therapy in hepatocellular carcinoma. Biochem Pharmacol. 2010;80:550–60.
2. Yang Y, Jin C, Li H, He Y, Liu Z, Bai L, *et al.* Improved radiosensitizing effect of the combination of etanidazole and paclitaxel for hepatocellular carcinoma in vivo. Exp Ther Med. 2012;3:299–303.
3. Wagner E. Programmed drug delivery: nanosystems for tumor targeting. Expert Opin Biol Ther. 2007;7:587–93.
4. Danhier F, Feron O, Préat V. To exploit the tumor microenvironment: passive and active tumor targeting of nanocarriers for anticancer drug delivery. J Control Release. 2010;148:135–46.
5. Xu Z, Chen L, Gu W, Gao Y, Lin L, Zhang Z, *et al.* The performance of docetaxel-loaded solid lipid nanoparticles targeted to hepatocellular carcinoma. Biomaterials. 2009;30:226–32.
6. Motornov M, Roiter Y, Tokarev I, Minko S. Stimuli-responsive nanoparticles, nanogels and capsules for integrated multifunctional intelligent systems. Prog Polym Sci. 2010;35:174–211.
7. Volk T, Jähde E, Fortmeyer HP, Glüsenkamp KH, Rajewsky MF. pH in human tumour xenografts: effect of intravenous administration of glucose. Br J Cancer. 1993;68:492–500.
8. Mellman I. Endocytosis and molecular sorting. Annu Rev Cell Dev Biol. 1996;12:575–625.
9. Tian L, Bae YH. Cancer nanomedicines targeting tumor extracellular pH. Colloids Surf B. 2012;99:116–26.
10. Ganta S, Devalapally H, Shahiwala A, Amiji M. A review of stimuli-responsive nanocarriers for drug and gene delivery. J Control Release. 2008;126:187–204.
11. Duan C, Zhang D, Wang F, Zheng D, Jia L, Feng F, *et al.* Chitosan-g-poly(N-isopropylacrylamide) based nanogels for tumor extracellular targeting. Int J Pharm. 2011;409:252–9.
12. Kesisoglou F, Panmai S, Wu Y. Nanosizing—oral formulation development and biopharmaceutical evaluation. Adv Drug Deliv Rev. 2007;59:631–44.
13. Lee YH, Mei F, Bai MY, Zhao SL, Chen DR. Release profile characteristics of biodegradable-polymer-coated drug particles fabricated by dual-capillary electrospray. J Control Release. 2010;45:58–65.
14. Enayati M, Chang MW, Bragman F, Edirisinghe M, Stride E. Electrohydrodynamic preparation of particles, capsules and bubbles for biomedical engineering applications. Colloids Surf A. 2011;382:154–64.
15. Wu YQ, Clark RL. Controllable porous polymer particles generated by electrospraying. J Colloid Interface Sci. 2007;310:529–35.
16. Chakraborty S, Liao IC, Adler A, Leong KW. Electrohydrodynamics: a facile technique to fabricate drug delivery systems. Adv Drug Deliv Rev. 2009;61:1043–54.

17. Ding LN, Lee T, Wang CH. Fabrication of monodispersed taxol-loaded particles using electrohydrodynamic atomization. J Control Release. 2005;102:395–413.
18. Wu YQ, MacKay JA, McDaniel JR, Chilkoti A, Clark RL. Fabrication of elastin-like polypeptide nanoparticles for drug delivery by electrospraying. Biomacromolecules. 2009;10:19–24.
19. Venditto VJ, Simanek EE. Cancer therapies utilizing the camptothecins: a review of the in vivo literature. Mol Pharm. 2010;7:307–49.
20. Chen Z, Cai XJ, Yang Y, Wu GN, Liu YW, Chen F, *et al.* Promoted transfection efficiency of pDNA polyplexes-loaded biodegradable microparticles containing acid-labile segments and galactose grafts. Pharm Res. 2012;29:471–82.
21. Cui WG, Qi MB, Li XH, Huang SZ, Zhou SB, Weng J. Electrospun fibers of acid-labile biodegradable polymers with acetal groups as potential drug carriers. Int J Pharm. 2008;361:47–55.
22. Deng XM, Li XH, Yuan ML, Xiong CD, Huang ZT, Jia WX, *et al.* Optimization of preparative parameters for poly-DL-lactide-poly(-ethylene glycol) microspheres with entrapped Vibrio cholera antigens. J Control Release. 1999;58:123–31.
23. Luo XM, Xu GS, Song HX, Yang SX, Yan SL, Jia GQ, *et al.* Promoted antitumor activities of acid-labile electrospun fibers loaded with hydroxycamptothecin via intratumoral implantation. Eur J Pharm Biopharm. 2012;82:545–53.
24. Liu J, Jiang ZZ, Zhang SM, Saltzman WM. Poly(ω-pentadecalactone-co-butylene-co-succinate) nanoparticles as biodegradable carriers for camptothecin delivery. Biomaterials. 2009;30:5707–19.
25. Zhang SL, Kawakami K, Yamamoto M, Masaoka Y, Kataoka M, Yamashita S, *et al.* Coaxial electrospray formulations for improving oral absorption of a poorly water-soluble drug. Mol Pharm. 2011;8:807–13.
26. Win KY, Feng SS. Effects of particle size and surface coating on cellular uptake of polymeric nanoparticles for oral delivery of anticancer drugs. Biomaterials. 2005;26:2713–22.
27. Jaworek A. Micro- and nanoparticle production by electrospraying. Powder Technol. 2007;176:18–35.
28. Mu L, Feng SS. Vitamin E TPGS used as emulsifier in the solvent evaporation/extraction technique for fabrication of polymeric nanospheres for controlled release of paclitaxel (Taxol®). J Control Release. 2002;80:129–44.
29. Derakhshandeh K, Erfan M, Dadashzadeh S. Encapsulation of 9-nitrocamptothecin, a novel anticancer drug, in biodegradable nanoparticles: factorial design, characterization and release kinetics. Eur J Pharm Biopharm. 2007;66:34–41.
30. Vauthier C, Bouchema K. Methods for the preparation and manufacture of polymeric nanoparticles. Pharm Res. 2009;26:1025–58.
31. Wang L, Li C. pH responsive fluorescence nanoprobe imaging of tumors by sensing the acidic microenvironment. J Mater Chem. 2011;21:15862–71.
32. Miura H, Onishi H, Sasatsu M, Machida Y. Antitumor characteristics of methoxypolyethylene glycol–poly(DL-lactic acid) nanoparticles containing camptothecin. J Control Release. 2004;97:101–13.
33. Dora CL, Alvarez-Silva M, Trentin AG, de Faria TJ, Fernandes D, da Costa R, *et al.* Evaluation of antimetastatic activity and systemic toxicity of camptothecin loaded microspheres in mice injected with B16-F10 melanoma cells. J Pharm Pharm Sci. 2006;9:22–31.
34. Smallbone K, Gavaghan DJ, Gatenby RA, Maini PK. The role of acidity in solid tumour growth and invasion. J Theor Biol. 2005;235:476–84.
35. Zhang LY, Yang M, Wang Q, Yuan L, Guo R, Jiang XQ, *et al.* 10-Hydroxycamptothecin loaded nanoparticles: preparation and antitumor activity in mice. J Control Release. 2007;119:153–62.
36. Hu ZL, Guo XQ, Yu Q, Qiu L, Li JZ, Ying K, *et al.* Down-regulation of adenine nucleotide translocase 3 and its role in camptothecin-induced apoptosis in human hepatoma QGY7703 cells. FEBS Lett. 2009;583:383–8.
37. Li XL, Zhen DH, Lu XW, Xu HE, Shao Y, Xue QP, *et al.* Enhanced cytotoxicity and activation of ROS-dependent c-Jun NH_2-terminal kinase and caspase-3 by low doses of tetrandrine-loaded nanoparticles in Lovo cells–A possible Trojan strategy against cancer. Eur J Pharm Biopharm. 2010;75:334–40.
38. Oh KS, Song JY, Cho SH, Lee BS, Kim SY, Kim K, *et al.* Paclitaxel-loaded pluronic nanoparticles formed by a temperature-induced phase transition for cancer therapy. J Control Release. 2010;148:344–50.
39. Li SD, Huang L. Pharmacokinetics and biodistribution of nanoparticles. Mol Pharm. 2008;5:496–504.
40. Maeda H. The enhanced permeability and retention (EPR) effect in tumor vasculature: the key role of tumor-selective macromolecular drug targeting. Adv Enzym Regul. 2001;41:189–207.
41. Moghimi SM, Hunter AC, Murray JC. Long-circulating and target-specific nanoparticles: theory to practice. Pharmacol Rev. 2001;53:283–318.
42. Ogston KN, Miller ID, Payne S, Hutcheon AW, Sarkar TK, Smith I, *et al.* A new histological grading system to assess response of breast cancers to primary chemotherapy: prognostic significance and survival. Breast. 2003;12:320–7.
43. Rodríguez-Hernández A, Brea-Calvo G, Fernández-Ayala DJM, Cordero M, Navas P, Sánchez-Alcázar JA. Nuclear caspase-3 and capase-7 activation, and poly(ADP-ribose) polymerase cleavage are early events in camptothecin-induced apoptosis. Apoptosis. 2006;11:141–59.